



Ephrin/Eph receptor interaction facilitates macrophage recognition of differentiating human erythroblasts

by Lea A. Hampton-O'Neil, Charlotte E. Severn, Stephen J. Cross, Sonam Gurung, Catherine D. Nobes, and Ashley M. Toye

Haematologica 2019 [Epub ahead of print]

Citation: Lea A. Hampton-O'Neil, Charlotte E. Severn, Stephen J. Cross, Sonam Gurung, Catherine D. Nobes, and Ashley M. Toye. Ephrin/Eph receptor interaction facilitates macrophage recognition of differentiating human erythroblasts.

Haematologica. 2019; 104:xxx

doi:10.3324/haematol.2018.215160

Publisher's Disclaimer.

E-publishing ahead of print is increasingly important for the rapid dissemination of science. Haematologica is, therefore, E-publishing PDF files of an early version of manuscripts that have completed a regular peer review and have been accepted for publication. E-publishing of this PDF file has been approved by the authors. After having E-published Ahead of Print, manuscripts will then undergo technical and English editing, typesetting, proof correction and be presented for the authors' final approval; the final version of the manuscript will then appear in print on a regular issue of the journal. All legal disclaimers that apply to the journal also pertain to this production process.

Ephrin/EPH receptor interaction facilitates macrophage recognition of differentiating human erythroblasts

Lea A. Hampton-O'Neil^{1,2,3}, Charlotte E. Severn^{1,2,3}, Stephen J. Cross^{1,4}, Sonam Gurung¹, Catherine D. Nobes¹, Ashley M. Toye^{*1,2,3}

¹School of Biochemistry, Biomedical Sciences Building, University of Bristol, University Walk, Bristol, BS8 1TD, UK. ²Bristol Institute for Transfusion Sciences, NHS Blood and Transplant, Filton, Bristol, BS34 7QH. ³National Institute for Health Research (NIHR) Blood and Transplant Unit in Red Blood Cell Products, University of Bristol, Bristol, BS8 1TD.

⁴Wolfson Bioimaging Facility, Biomedical Sciences Building, University of Bristol, University Walk, Bristol, BS8 1TD.

*Corresponding author:

Dr Ashley Toye

School of Biochemistry

Biomedical Sciences Building

University Walk

Bristol

BS8 1TD

Tel: 44 (0)117 3312111

Correspondence: ash.m.toye@bristol.ac.uk

Short Title

EPHB4 drives macrophage-erythroblasts interactions

Word count: 4027

Abstract word count: 188

Figure count: 6

Reference count: 42

Supplemental file: 1

Key Point

- EPHB4 and EPHB6 are essential for cell-cell recognition in erythroblastic island formation, independent of integrin activation
- Image analysis can be used to screen the role of receptors in erythroblastic islands and could have utility in the study of pathological erythropoiesis

Abstract

Erythropoiesis is one of the most efficient cellular processes in the human body producing approximately 2.5 million red blood cells every second. This process occurs in a bone marrow niche comprised of a central resident macrophage surrounded by differentiating erythroblasts, termed an erythroblastic island. It is not known what initially attracts the macrophage to erythroblasts to form these islands. The ephrin/EPH receptor family are known to regulate heterophilic cell-cell adhesion. We find that human VCAM1⁺ and VCAM1⁻ bone marrow macrophages and *in vitro* cultured macrophages are ephrin-B2 positive, whereas differentiating human erythroblasts express EPHB4, EPHB6 and EPHA4. Furthermore, we detect a rise in integrin activation on erythroblasts at the stage at which the cells bind which is independent of EPH receptor presence. Using a live cell imaging assay, we show that specific inhibitory peptides or shRNA depletion of EPHB4 cause a significant reduction in the ability of macrophages to interact with erythroblasts but does not affect integrin activation. This study demonstrates for the first time that EPHB4 expression is required on erythroblasts to facilitate the initial recognition and subsequent interaction with macrophages, alongside the presence of active integrins.

Introduction

Erythropoiesis is the process whereby haematopoietic stem cells (HSC) develop, undergoing multiple stages of cell division and differentiation before enucleating to form nascent reticulocytes. In humans, this process occurs in the bone marrow. HSCs undergo asymmetric division and lineage restriction to form pro-erythroblasts in the HSC niche, where they bind a macrophage to form a specialised niche called an erythroblastic island. This niche is formed by a central resident macrophage which is surrounded by differentiating erythroblasts¹. The erythroblastic island is important for proliferation and terminal differentiation of erythroid cells, as macrophages are thought to supply nutrients to the surrounding erythroid cells, promote growth through survival signals and phagocytose the pyrenocyte after enucleation²⁻⁴.

Multiple receptors are present on the surface of macrophages and erythroblasts which are involved in erythroblastic island interactions. These include intercellular adhesion molecule 4 (ICAM4), vascular cell adhesion molecule 1 (VCAM1), erythroblast-macrophage protein (Emp), Fms related tyrosine kinase 3 (Flt3), proto-oncogene tyrosine-protein kinase MER (Mer-TK), dystroglycan (DG) receptor, integrins and EPH receptors⁴⁻¹⁰. It has already been established that ICAM4^{-/-} mice formed significantly less erythroblastic islands than control mice⁶ and the loss of erythroblast-macrophage protein (Emp) in mice leads to apoptosis of erythroid precursors and enucleation failure^{5,11}. Finally, integrin β 3 knockout mice have a higher amount of early erythroblast release from erythroblastic islands⁷. Overall, although we now know more about the importance of certain receptors for erythroblastic island integrity in mice, we do not know exactly which receptors are involved in the formation and maintenance of human erythroblastic islands or how these two different cell types specifically recognise one another as binding partners.

The EPH receptor family is the largest tyrosine kinase receptor family¹². It is separated into two protein branches which are largely distinct: the A family and the B family¹³. EPH receptors are very versatile as they can control adhesion, migration and proliferation^{12,14,15}, leading to their important role in development; in particular through their role in contact inhibition of locomotion (CIL). One current model for CIL suggests that depending on which EPH receptors and their ligands ephrins are present and their abundance at the surface will dictate the response of cells as they come into contact¹⁶. As both EPHB and EPHA receptors can be simultaneously expressed on the surface of cells, it is thought that the ratio of EPHA to EPHB receptor abundance at the surface of the cells determines the behaviour of the two cells as they collide^{16,17}. Hence, when EPHA receptors are in excess and engage the ligand, the cells will be repulsed, whereas if EPHB are in excess and activated, this can lead to attraction and possibly drive adhesion.

Recently, several reports have discussed the importance of EPH receptor function within the bone marrow niche. In mice, one EPHB4 ligand, ephrin-B2 is expressed on HSCs and is important for the release of the progenitor cells into the bloodstream^{14,18}. EPHB4 is also reported to exert control over niche size, as transgenic mice that overexpress EPHB4 produce more HSC cells and display a higher bone marrow reconstitution capacity^{19,20}. However, the role that EPH receptors play specifically in the erythroid lineage is based primarily upon the demonstration of EPHB4 expression on human bone marrow CD34⁺ cells and from the observed increase in CFU-E formation upon co-culture with stromal cells overexpressing ephrin-B2 or HSCs overexpressing EPHB4²¹⁻²³. More recently, Anselmo et al. (2016) proposed a role for EPHB1 in the activation of integrins via an agrin-dependent pathway in mice and hypothesised that this facilitates erythroblast binding to macrophages. Whether this observation extends to a human macrophage island context is unknown.

We find that for humans, EPHB4, EPHB6 and EPHA4 are the only EPH receptors present on erythroblasts and that these proteins are differentially expressed on the surface during terminal differentiation. Specifically, we found high EPHB4 and EPHB6 expression in the early stages of erythropoiesis, and by the reticulocyte stage, only EPHA4 is detected. We also demonstrate that during the expansion phase where EPHB4 and EPHB6 are highly expressed, erythroblasts also have an increase in active integrin. Using live cell imaging we show that the inhibition of EPHB4 interaction with ephrin-B2 results in a decrease in the association between erythroblasts and macrophages despite the continued presence of active integrins. This work demonstrates for the first time that ephrin/Eph interactions, as well as the presence of integrins, drive the recognition between macrophages and erythroblasts during human erythroblastic island formation.

Methods

Bone marrow isolation

Bone marrow aspirate samples were provided by Dr Michael Whitehouse (University of Bristol) with informed consent for research use. The use of donated bone marrow was approved by the Bristol Research Ethics Committee (REC Number 12/SW/0199). Cells were washed from a universal sample tube using HBSS (Sigma-Aldrich) containing 0.6% acid citrate dextrose (ACD) to remove the heparin-coated beads (included to prevent coagulation). The red pulp was macerated onto a 70µm filter. Cells were washed once more with HBSS and ACD and centrifuged at 300g between washes. Red cells were lysed using red cell lysis buffer (155mM NH₄Cl, 0.137mM EDTA, 1mM KHCO₃, pH 7.5) for 10 minutes on ice, cells were washed a further time in HBSS with ACD, counted and stored until required.

FACS

Mononuclear cells (MNCs) were thawed and washed twice with PBS with 1% BSA and 2% glucose (PBSAG). CD14⁺ isolation was performed on thawed bone marrow MNCs according to manufacturers' instructions (Miltenyi Biotech). Cells were counted and resuspended in PBSAG and CD14-Pacific Blue, CD106-PE and CD169-APC antibodies were added for 30 minutes at 4°C in the dark. The cells were washed twice in PBSAG and then the CD14⁺CD106⁺ and CD14⁺CD106⁻ populations were sorted using a BD Influx Cell Sorter.

Live Cell Imaging

Macrophages were grown for 7 days, as described above, in a 24 well plate (Corning, Corning, New York, US). At day 7, cells were labelled with Cell Tracker Green CFMDA (Thermo Fisher) following manufacturer's instructions. For bone marrow macrophages, the labelling was conducted immediately after sorting. Erythroblasts on day 6 of expansion were added to the macrophages and left overnight in culture media (IMDM (Gibco), 3%v/v Human serum (Sigma-Aldrich), 10U/mL erythropoietin (Roche, Basel, Switzerland) and 1mg/mL holotransferrin (Sanquin)). The biotinylated TNYLFSPNGPIARAWGSGSK-Biotin (TNYL), EILDVPSTGSGSK-Biotin (EIL) and the control peptide DYP SMAMYSPVSGSGSK-Biotin (DYP) were synthesized by Cambridge Peptides UK (Birmingham, UK) and added where indicated. The media was changed the next day with phenol-red free imaging media with replenished peptides where indicated. The optimal final ratio of cells used was 2 erythroblasts to 1 macrophage to prevent overcrowding. The plate was imaged using Incucyte (Essen BioScience, Welwyn Garden City, UK) every hour at 20x magnification. The spatial relationship between erythroblasts and macrophages was characterised using Fiji^{24,25}. Initially, lateral drift in the phase-contrast and fluorescence images over time was corrected using the StackReg plugin²⁶. A difference of Gaussian filter (approximating the equivalent Laplacian of Gaussian²⁷) was then applied to the phase-contrast channel to enhance features with diameters matching those expected for erythroblasts. Erythroblasts were subsequently identified with the TrackMate plugin using the Laplacian of Gaussian feature detector²⁸. Fluorescence channel images were processed with rolling-ball and Gaussian filters to remove inhomogeneity of illumination and high-frequency noise, respectively. The images were then thresholded using the Otsu method²⁹ with a user-defined fixed multiplier offset and passed through the ImageJ particle analyser to identify macrophages. Macrophages were tracked between frames using the Apache HBase (v1.3.1; Apache Software Foundation, <https://hbase.apache.org>) implementation of the Munkres algorithm with costs assigned based on object centroid separation³⁰. Instances where objects in the phase-contrast channel coincided with macrophages identified in the fluorescence channel were removed, as these likely corresponded to accidental detection of macrophages. Finally, spatial relationships between

erythroblasts and macrophages were determined based on the maximum separation of object perimeters. Multiple erythroblasts could be assigned to a single macrophage. This program can be found at doi: 10.5281/zenodo.3237585 (Stephen Cross. (2018, March 14). SJCross/RelateCells v1.2.2 (Version v1.2.2). Zenodo.).

Antibodies, cell culture, transduction, RT-PCR, western blotting, flow cytometry, cytopins and statistics

All these methods can be found in the Supplementary Methods.

Results

Ephrin-B2 is expressed by M2-like macrophages and bone marrow macrophages

As reported previously by Heideveld et al. (2017), macrophages treated with dexamethasone (+Dex) phenotypically resemble the resident macrophages found in bone marrow and foetal liver³¹, exhibiting a high level of CD163 and CD169, similar to bone marrow macrophages (Figure S1). Furthermore, these cultured macrophages are known to be able to help the erythroblasts expand^{32,33}, form erythroblastic islands and phagocytose nuclei³¹. However, whereas up to 70% of bone marrow isolated CD14⁺CD16⁺ macrophages are VCAM1⁺, +Dex macrophages are VCAM1⁻. It is known that bone marrow stromal cells, including macrophages, express ephrinB2²³. Figure 1A and 1B confirm that all three macrophage types, +Dex *in vitro* cultured, VCAM1⁺ and VCAM1⁻ bone marrow macrophages express ephrin-B2, the most potent receptor for EPHB4 and EPHB6 receptors (see below). There was no discernible difference between the expression levels of ephrin-B2 on sorted VCAM1⁺ and VCAM1⁻ macrophages but the *in vitro* culture +Dex macrophages express higher levels (Figure 1C).

EPHB4, EPHB6 and EPHA4 are expressed in expanding and differentiating erythroblasts

To determine which EPH receptors are expressed in erythroblasts at different stages of development, RT-PCR was performed on 3 independent *in vitro* cultured differentiation courses. In these cultures, CD34⁺ cells are isolated and expanded for 8 days, called D0 to D7. During this time, the cells express CD34 and CD36, markers of the BFU-E and CFU-E. The cells are then differentiated for 8 days, called T0 to T168. These stages of differentiation can be separated by their morphology using cytopins (Figure S2A and B). EPHB4, EPHB6 and EPHA4 mRNAs were expressed in expanding day 6 and differentiating T0, representing the proerythroblast/basophilic stage in our culture system. As shown in Figure 1D, RNA for numerous EPH receptors (EPHA1, EPHA2, EPHA3, EPHA6, EPHA7, EPHA8, EPHB2 and EPHB3) was not detected during erythropoiesis. Western blots confirmed EPHB4, EPHB6 and EPHA4 protein expression (Figure 1E). EPHA4 expression diminished but was still retained at the

reticulocyte stage. Unlike in mice⁹, EPHB1 was not reproducibly detected at either the RNA or protein level (being detected by RT-PCR only once in 4 separate erythroid differentiation courses). Interestingly, the ligand ephrin-B2 is also present in the late stage of expansion in erythroblasts.

Erythroblast surface expression of EPH receptors is dynamic during terminal differentiation

To assess the timeframe in which the EPH receptors are expressed on the surface of erythroblasts during differentiation, a surface binding assay was performed. Ephrin-B2 was chosen as the ligand used in this experiment as it binds all EPHB receptors³⁴. Ephrin-B2 was clustered with a fluorescently-conjugated IgG antibody and added to the live cells. Figure 1F demonstrates that the cells bind ephrin-B2-Fc during the final part of the expansion phase (D5 and D6) when cells are CD34^{low}/CD36^{high} proerythroblasts (Figure 2A). As cells commence terminal differentiation (T0 hours), there is a steady reduction of ligand binding (no statistically significant binding after T0), and by T72 hours all binding is lost. At T72 hours, the majority of erythroblasts present in culture are beyond the basophilic stage (Figure S2A), confirming that EPHB receptors are expressed during the early phases of terminal differentiation.

Integrins are crucial in cell-cell contact and adhesion with macrophages through the formation of focal adhesion points^{6,7,9,35}. Therefore, we tested whether the appearance of integrins on the erythroblast surface coincided with EPHB4 receptor surface expression. To detect integrins, a surface binding experiment was conducted using VCAM1-Fc where the integrins were pre-activated with manganese to ensure VCAM1-Fc construct binding. Without pre-activation, no binding was found (Figure S3), but when all the integrins were activated, VCAM1-Fc bound throughout erythroblast differentiation until approximately T144 hours when 50% of the cells were reticulocytes (Figure 1F). Manganese treatment was observed to increase cell death and clustering. Therefore flow cytometry analysis was performed only on live single cells during the surface assay by gating on unclustered propidium iodide negative cells.

Baseline activation of integrins occurs during the height of EPHB4 and EPHB6 expression

We next wanted to establish the level of integrin activation during the stages at which EPHB4/B6 become more pronounced at the surface of erythroblasts. To do this, we used an antibody that specifically recognises the active form of integrin $\beta 1$, which is present in both the VLA-4 (integrin $\alpha 4\beta 1$) and VLA-5 (integrin $\alpha 5\beta 1$) complexes. Manganese was used to activate integrins beforehand as a positive control. We detected a marked increase of integrin activation in a small percentage of the cells between Days 4 and 5 on erythroblasts in the absence of any treatment (representing an

increase in 10 to 30% of cells at Day 5 and 90% at Day 6; Figure 2B). This increase represents 50% of MFI of that observed with the manganese treatment, which activates all the integrins (Figure 2C). The CD36^{high}/CD34^{low/-} populations displayed this rise in baseline integrin activation (Figure 2A).

To establish the effects of EPH receptor stimulation on integrin activation, the amount of active form of integrin β 1 was monitored in the presence of clustered ephrin-B2. EPH receptor engagement, surprisingly, had no significant effect on the level of activation of integrin β 1 (Figure 2B).

Peptide inhibition of EPHB4 activation impacts on macrophage-erythroblast interactions

The EPHB4 receptor inhibitor (TNYL-RAW peptide) competes selectively with ephrin-B2 binding to EPHB4 but does not activate the receptor³⁶. In a competition assay, it was observed that addition of EPHB4 inhibitor caused a significant decrease in ephrin-B2 binding to the cells at day 5, with a marked decrease at day 4 as well, but this did not occur using the DYP control peptide (Figure 2D). This effect on ephrin-B2 binding did not have an effect on the rise in integrin β 1 activation (Figure 2E).

Using a live cell imaging assay described recently in Heideveld et al. (2017) and further developed in Figure S4, the role of the EPH receptor in macrophage-erythroblast interaction was interrogated in the presence or absence of inhibitory peptide (Figure 3A). The number of interactions an individual macrophage makes with erythroblasts in each image frame is referred to as links. Images were taken every hour to screen as many conditions as possible on the Incucyte and ensure comparability. The box plots in Figure 3B and C demonstrate that the addition of the EPHB4 inhibitor TNYL-RAW significantly reduced the average number of interactions (50% vs 75% macrophage with more than 1 link on average; $p < 0.0001$) but not the mean duration of these contacts. Importantly, the movement of the macrophages was not affected by the addition of inhibitors, as +Dex macrophages still exhibit a high degree of movement with each peptide treatment (Figure 3D and E).

Although +Dex macrophages do not express VCAM1, we also tested whether other integrin interactions contribute to the macrophage-erythroblast relationship in addition to EPHB4. An inhibitory peptide designed against VLA-4, EIL peptide, was introduced in the formation assay³⁷. This peptide was generated from a fragment of fibronectin which binds and locks the integrin β 1 into the active form. The presence of the VLA-4 inhibitor in the formation assay led to a loss in mean duration (75% of cells have contacts which last less than 1h compared to 75% which last more) and an average number of links in +Dex cells (Figure 3B and C).

EPHB4 depletion using shRNA impacts macrophage-erythroblast interaction

To assess the specific importance of EPH receptor expression and rule out secondary binding of the inhibitory peptides, EPHB4 and EPHB6 were depleted individually using lentiviral shRNA transduction of early erythroblasts. When EPHB4 is silenced, we observed that there is a concomitant loss of EPHB6 (Figure 4A). This was not a reciprocal relationship, as EPHB6 depletion did not reduce the level of EPHB4 expression, as can be observed in Figure 4B. Heterodimerization of EPHB6 with EPHB4 may, therefore, be important for its stability on the erythroblast surface but not vice versa³⁸. This happened in the presence of two different shRNAs for each protein (data not shown). Importantly, depletion of EPHB4 reduced ephrin-B2 binding in a surface binding assay but not when EPHB6 alone was knocked down suggesting that EPHB4 is responsible for the majority of ephrin-B2 binding (Figure 4C). As was seen with the inhibitors, the depletion of the EPHB receptors did not lead to a reduction in integrin $\beta 1$ activation (Figure 4D). Therefore, integrin activation at the surface of proerythroblasts is not due to the presence or activation of EPHB4.

When EPHB knockdown erythroblasts were added to +Dex macrophages, only erythroblasts with EPHB4 depletion caused a loss of both average number of links (scrambled control median of 0.43 vs EPHB4 KD median of 0.26) and the mean duration of these contacts between +Dex macrophages (75% last longer than 1h in scrambled control vs 50% in EPHB4 KD on average). The loss of EPHB6 did not lead to any differences in mean duration to the scrambled control (Figure 4E and F); therefore, confirming the EPHB4 peptide inhibitor result. Interestingly, EPHB6 knockdown leads to a statistically higher number of contacts (median of 0.43 vs 0.57; $p < 0.0001$); indicating that the sole presence of EPHB4 is enough to have a higher number of long-lasting contacts with macrophages. It should be noted knockdown experiments are less sensitive to the macrophage:erythroblast ratio than the peptide experiments, probably due to peptide saturation occurring.

Primary bone marrow macrophages also require EPHB4 expression on erythroblasts for interaction

To extend a role for ephrin interactions to *ex vivo* bone marrow macrophages, erythroblastic islands were reconstituted using human bone marrow aspirates. VCAM1⁺ and VCAM1⁻ macrophage populations were isolated in a two-stage process, first by isolating CD14⁺ cells using magnetic beads and then sorting for CD14⁺ VCAM1⁺ cells (Figure 5A). Flow cytometry confirmed that VCAM1⁺ cells were also CD169⁺ as described previously (Chow et al., 2013; Figure S1). Erythroblasts cultured from CD34⁺ cells were then introduced at the same stage as for the +Dex macrophages in earlier experiments. Clusters of cells composed of macrophages and erythroblasts were observed following this method of reconstitution (Figure 5B and Figure S5). Furthermore, these macrophages are highly motile as witnessed for the +Dex macrophages (Figure 5C) and by Belay et al. (2017). In Figure 5D

and E, VCAM1⁺ bone marrow macrophages have long-lasting interactions with multiple erythroblasts. VCAM1⁻ bone marrow macrophages have 50% of contacts lasting more than 1h compared to 75% of VCAM1⁺ cells. Furthermore, VCAM1⁻ cells form statistically fewer links ($p < 0.0001$). Therefore, as demonstrated with +Dex macrophages, a lack of VCAM1 does not stop interactions with erythroblasts, but its presence does indicate a macrophage with a subtly enhanced erythroblast binding ability.

Importantly, the results with VCAM1⁺ and VCAM1⁻ cells reproduced those observed using +Dex cultured macrophages with the loss of EPHB4 impacting on erythroblast association. However, unlike +Dex cultured macrophages the loss of EPHB6 also significantly affected the initiation of associations between bone marrow macrophages and erythroblasts. Therefore, EPHB6 appears to be as equally important as EPHB4 in erythroblastic island reconstitutions when bone marrow macrophages are used (Figure 5D and E). These results cement the importance of EPHB receptors' presence at the same time as active integrins for the recognition of erythroblasts as binding partners by macrophages.

Discussion

This work has used an imaging-based assay to interrogate the importance of EPH receptor interactions in the initial association between macrophages and erythroblasts. We have demonstrated that EPHB receptors are present at the surface of erythroblasts during terminal differentiation between the proerythroblast and orthochromatic stages and that this temporal expression profile coincides with increased integrin activation (Figures 1 and 2). The depletion of EPHB4 causes macrophages and erythroblasts to have fewer long-duration contacts, and the removal of EPHB4 or its inhibition had no effect on integrin activation (Figures 4 and 5). Therefore, loss of EPHB4 alone is sufficient to reduce macrophage recognition of erythroblasts as binding partners. We, therefore, suggest ephrin-B2 binding alongside integrin activation reinforces recognition. As illustrated in Figure 6, we, therefore, propose a new model of interaction whereby EPHB receptors and integrin engagement act in concert as a coincidence detector, to ensure that the macrophage associates and binds to the differentiating progenitor cell at the appropriate time.

Furthermore, contact inhibition of locomotion is thought to be controlled by a ratio of EPHB and EPHA receptors¹⁶. Interestingly, we observed that erythroblasts have a high level of EPHB and EPHA receptors during early stages of differentiation but lose EPHB receptors by the final stages of differentiation, while EPHA is retained (albeit at lower levels). We hypothesise that EPH receptors may contribute throughout the whole process of differentiation; in the early stages of differentiation, EPHB receptor is present in higher amounts than EPHA leading to recognition between the cells,

supported by the EPHB4 inhibition disrupting this interaction. As the cells differentiate, the amount of EPHA receptor becomes dominant over EPHB, tantalisingly suggesting that once the erythroblast has enucleated to form a reticulocyte EPHA4 may be involved in the separation of the cells, a hypothesis that will need to be explored in future experiments.

It is notable that in humans EPH receptor activation did not affect integrin activation at day 5, which contradicts the findings of a recent report⁹, which showed that in mice EPHB1 receptor engagement caused a rise in CD29 and its activation at the surface of erythroblasts after agrin treatment. We cannot exclude the possibility that agrin still has a role in the integrin β 1 activation observed in this study, separate from its additional role in activating the EPHB receptors at the surface. However, our results indicate that these two events are likely independent and that the difference between the previous study and ours is due to species differences.

Our observation here that VCAM1⁻ macrophages are capable of interacting with erythroblasts confirms work by Wei & Frenette⁴¹ and Falchi et al.³³. All three types of macrophages tested in this study were capable of binding erythroblasts to some degree. This change in the level of binding could be related to the subtle changes which exist between these cells, be it the presence of VCAM1, different levels of ephrin-B2 at their surface or other unknown differences. Indeed, it is known that varying levels of ephrin-B2 can influence the function of EPHB6⁴². As the bone marrow macrophages express lower amounts of ephrin-B2 expression than cultured macrophages, this may explain the former's interaction sensitivity to EPHB6 silencing. Taken together, the experiments have shown that EPH receptors are more important to the recognition between erythroblasts and macrophages than VCAM1. This mirrors the results found by Wei and Frenette who reported that EMP is more important than VCAM1 for the further stages of the interaction⁴¹. However, we do not fully understand the hierarchy between EPH receptors and the integrins. Our experiments do however demonstrate that both EPH and integrins together are essential for the interaction and recognition of the macrophages to the erythroblasts.

The evidence presented here also suggests a VCAM1-independent interaction for integrins in erythroblastic island formation, or perhaps associations are more promiscuous than anticipated. In addition, although a large number of mature macrophages in the human bone marrow are VCAM1⁺, indicating a preference for this phenotype in island formation, the ability for VCAM1⁻ macrophages to form interactions with erythroblasts indicates a flexibility in terms of the type of macrophages which can participate in erythroblastic island formation which may be important during stress erythropoiesis. VCAM1's role in helping erythroblasts expand⁴⁰ would explain this preference.

In addition to driving interactions, the EPH receptors may play additional supportive roles within the erythroblastic island. It was previously reported that overexpression of EPHB4 increases HSC numbers²⁰, therefore EPHB4 might have a proliferative role within the niche. Finally, the observation that erythroblasts express both ephrin-B2 and EPHB4, raises the potential for homophilic cell interaction that could lead to higher proliferation and also explains the ability of erythroblasts to proliferate *in vitro* in the absence of macrophages.

In summary, it has previously been difficult to determine the specific contribution certain receptors play in human macrophage-erythroblast interactions during erythropoiesis. This study has successfully employed live imaging of human macrophages and erythroblasts to probe the role of a potential receptor interaction between the cells over time. This has shown a dependence on EPHB interactions for the macrophage and erythroblast interaction for the first time, and we believe this imaging assay can help further delineate the importance of other receptors in the interaction between erythroblasts and macrophages in future experiments.

Acknowledgement

We would like to thank Dr. Emile van den Akker for discussion on development of an antibody panel for macrophages; Dr. Andrew Herman and Lorena Sueiro for the FACS; the Wolfson Bioimaging facilities for access to the Incucyte, widefield and all their help; Abi Gartner for his help with analysis. We thank the Elizabeth Blackwell Institute Wellcome Trust ISSF Award for providing funding for Stephen Cross. This work was funded by NHS Blood and Transplant R&D grants (WP15-05); a Wellcome Trust PhD studentship (LHO-N; 105385/Z/14/Z). This study/project is also funded by/supported by the National Institute for Health Research (NIHR) Blood and Transfusion Research Unit (NIHR BTRU) in Red Cell Products (NIHR-BTRU-2015-10032).

The views expressed are those of the author(s) and not necessarily those of the NIHR or the Department of Health and Social Care.

Author contributions

LH-ON and AMT designed the experiments. LH-ON conducted the majority of the experimental work. SJC developed and optimised the image analysis programme. SG conducted experiments. CS optimised the macrophage differentiation cultures, conducted experiments, edited the paper and produced figure 6. CN provided Eph/ephrin experimental advice. LH-ON and AMT wrote the paper. All authors read and edited the final version of the manuscript.

Disclosure of Conflicts of Interest

The authors declare no competing interests.

1

References

1. Socolovsky M. Exploring the erythroblastic island. *Nat Med.* 2013;19(4):399–401.
2. Hanspal M, Hanspal JS. The association of erythroblasts with macrophages promotes erythroid proliferation and maturation: a 30-kD heparin-binding protein is involved in this contact. *Blood.* 1994;84(10):3494–3504.
3. Rhodes MM, Kopsombut P, Bondurant MC, Price JO, Koury MJ. Adherence to macrophages in erythroblastic islands enhances erythroblast proliferation and increases erythrocyte production by a different mechanism than erythropoietin. *Blood.* 2007;111(3):1700–1708.
4. Toda S, Segawa K, Nagata S. MerTK-mediated engulfment of pyrenocytes by central macrophages in erythroblastic islands. *Blood.* 2014;123(25):3963–3971.
5. Soni S, Bala S, Gwynn B, Sahr KE, Peters LL, Hanspal M. Absence of Erythroblast Macrophage Protein (Emp) Leads to Failure of Erythroblast Nuclear Extrusion. *J Biol Chem.* 2006;281(29):20181–20189.
6. Lee G, Lo A, Short SA, et al. Targeted gene deletion demonstrates that the cell adhesion molecule ICAM-4 is critical for erythroblastic island formation. *Blood* 2006;108(6):2064–2071.
7. Wang Z, Vogel O, Kuhn G, Gassmann M, Vogel J. Decreased stability of erythroblastic islands in integrin $\beta 3$ -deficient mice. *Physiol Rep.* 2013;1(2):e00018.
8. Fraser ST, Midwinter RG, Coupland LA, et al. Heme oxygenase-1 deficiency alters erythroblastic island formation, steady-state erythropoiesis and red blood cell lifespan in mice. *Haematologica.* 2015;100(5):601–610.
9. Anselmo A, Lauranzano E, Soldani C, et al. Identification of a novel agrin-dependent pathway in cell signaling and adhesion within the erythroid niche. *Cell Death Differ.* 2016;23(8):1322–1330.
10. Jacobsen RN, Nowlan B, Brunck ME, Barbier V, Winkler IG, Levesque J-P. Fms-like tyrosine kinase 3 (Flt3) ligand depletes erythroid island macrophages and blocks medullar erythropoiesis in the mouse. *Exp Hematol.* 2016;44(3):207-212
11. Soni S, Bala S, Hanspal M. Requirement for erythroblast-macrophage protein (Emp) in definitive erythropoiesis. *Blood Cells Mol Dis.* 2008;41(2):141–147.
12. Kullander K, Klein R. Mechanisms and functions of Eph and ephrin signalling. *Nat Rev Mol Cell Biol.* 2002;3(7):475–486.

13. Pasquale EB. Eph receptors and ephrins in cancer: bidirectional signalling and beyond. *Nat Rev Cancer*. 2010;10(3):165–180.
14. Okubo T, Yanai N, Obinata M. Stromal cells modulate ephrinB2 expression and transmigration of hematopoietic cells. *Exp Hematol*. 2006;34(3):330–338.
15. Rutkowski R, Mertens-Walker I, Lisle JE, Herington AC, Stephenson SA. Evidence for a dual function of EphB4 as tumor promoter and suppressor regulated by the absence or presence of the ephrin-B2 ligand. *Int J Cancer*. 2012;131(5):E614–E624.
16. Astin J, Batson J, Kadir S, et al. Competition amongst Eph receptors regulates contact inhibition of locomotion and invasiveness in prostate cancer cells. *Nat Cell Biol*. 2010;12(12):1194–1204.
17. Alfaro D, Muñoz JJ, García-Ceca J, Cejalvo T, Jiménez E, Zapata AG. The Eph/ephrinB signal balance determines the pattern of T-cell maturation in the thymus. *Immunol Cell Biol*. 2011;89(8):844–852.
18. Kwak H, Salvucci O, Weigert R, et al. Sinusoidal ephrin receptor EPHB4 controls hematopoietic progenitor cell mobilization from bone marrow. *J Clin Invest*. 2016;126(12):4554–4568.
19. Tosato G. Ephrin ligands and Eph receptors contribution to hematopoiesis. *Cell Mol Life Sci*. 2017;74(18):3377–3394.
20. Nguyen TM, Arthur A, Panagopoulos R, et al. EphB4 Expressing Stromal Cells Exhibit an Enhanced Capacity for Hematopoietic Stem Cell Maintenance. *Stem Cells*. 2015;33(9):2838–2849.
21. Suenobu S, Takakura N, Inada T, et al. A role of EphB4 receptor and its ligand, ephrin-B2, in erythropoiesis. *Biochem Biophys Res Commun*. 2002;293(3):1124–1131.
22. Inada T, Iwama A, Sakano S, Ohno M, Sawada K, Suda T. Selective expression of the receptor tyrosine kinase, HTK, on human erythroid progenitor cells. *Blood*. 1997;89(8):2757–2765.
23. Wang Z, Miura N, Bonelli A, et al. Receptor tyrosine kinase, EphB4 (HTK), accelerates differentiation of select human hematopoietic cells. *Blood*. 2002;99(8):2740–2747.
24. Schneider CA, Rasband WS, Eliceiri KW. NIH Image to ImageJ: 25 years of image analysis. *Nat Methods*. 2012;9(7):671–675.
25. Schindelin J, Arganda-Carreras I, Frise E, et al. Fiji: An open-source platform for biological-

- image analysis. *Nat Methods*. 2012;9(7):676–682.
26. Thévenaz P, Ruttimann UE, Unser M. A pyramid approach to subpixel registration based on intensity. *IEEE Trans Image Process*. 1998;7(1):27–41.
 27. Marr D, Hildreth E. Theory of Edge Detection. *Proc R Soc B Biol Sci*. 1980;207(1167):187–217.
 28. Tinevez JY, Perry N, Schindelin J, et al. TrackMate: An open and extensible platform for single-particle tracking. *Methods*. 2017;11580–11590.
 29. Otsu N. A Threshold Selection Method from Gray-Level Histograms. *IEEE Trans Syst Man Cybern*. 1979;9(1):62–66.
 30. Munkres J. Algorithms for the Assignment and Transportation Problems. *J Soc Ind Appl Math*. 1957;5(1):32–38.
 31. Heideveld E, Hampton-O'Neil LA, Cross SJ, et al. Glucocorticoids induce differentiation of monocytes towards macrophages that share functional and phenotypical aspects with erythroblastic island macrophages. *Haematologica*. 2018;103(3):395-405.
 32. Heideveld E, Masiello F, Marra M, et al. CD14+ cells from peripheral blood positively regulate hematopoietic stem and progenitor cell survival resulting in increased erythroid yield. *Haematologica*. 2015;100(11):1396-1406.
 33. Falchi M, Varricchio L, Martelli F, et al. Dexamethasone targeted directly to macrophages induces macrophage niches that promote erythroid expansion. *Haematologica*. 2015;100(2):178–187.
 34. Zhou R. The Eph Family Receptors and Ligands. *Pharmacol Ther*. 1998;77(3):151–181.
 35. Eshghi S, Vogelezang MG, Hynes RO, Griffith LG, Lodish HF. Alpha4beta1 integrin and erythropoietin mediate temporally distinct steps in erythropoiesis: integrins in red cell development. *J Cell Biol*. 2007;177(5):871–880.
 36. Wang Y, Menendez A, Fong C, Elalieh HZ, Chang W, Bikle DD. Ephrin B2/EphB4 mediates the actions of IGF-I signaling in regulating endochondral bone formation. *J Bone Miner Res*. 2014;29(8):1900–1913.
 37. Spring FA, Parsons SF, Ortlepp S, et al. Intercellular adhesion molecule-4 binds $\alpha 4\beta 1$ and αv -family integrins through novel integrin-binding mechanisms. *Blood*. 2001;98(2):458–466.
 38. Kaenel P, Mosimann M, Andres AC. The multifaceted roles of Eph-ephrin signaling in breast cancer. *Cell Adh Migr*. 2012;6(2):138–147.

39. Chow A, Huggins M, Ahmed J, et al. CD169⁺ macrophages provide a niche promoting erythropoiesis under homeostasis and stress. *Nat Med*. 2013;19(March):429–436.
40. Belay E, Hayes BJ, Blau CA, Torok-Storb B. Human cord blood and bone marrow CD34⁺ cells generate macrophages that support erythroid islands. *PLoS One*. 2017;12(1):e0171096.
41. Wei Q, Frenette PS. Macrophage Erythroblast Attacher (MAEA), but Not VCAM1, Is Required for the Bone Marrow Erythroblastic Niche. *Blood*. 2015;126(23):2128.
42. Matsuoka H, Obama H, Kelly ML, Matsui T, Nakamoto M. Biphasic functions of the kinase-defective Ephb6 receptor in cell adhesion and migration. *J Biol Chem*. 2005;280(32):29355–29363.

Figure 1 - EPH receptor expression profile is specific to the cell type and its differentiation

A – Lysates from cultured macrophages, HeLa and HEK cells were western blotted for ephrin-B2 and GAPDH. This is a representative blot (n=3). B – Lysates from sorted VCAM⁺ and VCAM⁻ bone marrow CD14⁺ cells were blotted for ephrin-B2 and GAPDH. This is a representative blot (n=2). C – Lysates from HEK, HeLa, sorted bone marrow and cultured macrophages with dexamethasone were probed for ephrinB2 and GAPDH. This is a representative blot (n=2). D – Representative DNA gels showing the PCR products from an erythroblast differentiation course using primers against EPHA1-8 and EPHB1-6 (n=3). For each sample, a negative control was also performed to confirm the absence of genomic DNA contamination. HEK293, OVCAR 3 and HeLa cells were used as positive controls. E – Lysates from HeLa, HEK cells and an erythroblast differentiation course were blotted for EPHB4, EPHB6, EPAA4, ephrin-B2 and GAPDH. This is a representative blot (n=3). A, B, C and E - All lanes were loaded with 1x10⁶ cells. F - Graph showing the mean fluorescent intensity (MFI) obtained by flow cytometry of the ephrin-B2-Fc and VCAM-Fc constructs binding to erythroblasts throughout terminal differentiation. EB2 is ephrin-B2-Fc, and VCAM Mn is VCAM-Fc with manganese activation. The ephrin constructs were pre-clustered. All points are means for ephrin-Fc constructs (n=5) and VCAM (n=3). The error bars represent the standard error of the mean. Binding to the constructs was statistically compared to the IgG control using two-way ANOVA (***) (p<0.001); **** (p<0.0001)). The control for VCAM binding without manganese is in Figure S3.

Figure 2 – Activated Integrin β 1 on proerythroblasts is not affected by EPHB4 inhibition

A – Representative contour plot of the erythroblasts at different stages of expansion on days 3, 4 and 5 of culture (n=5). IgG is in red, and antibodies are in blue. B – Graph showing the percentage of cells with active integrin obtained by flow cytometry of these cells with the active form of integrin β 1 (clone HUTS-21) through days 3, 4 and 5 of erythroblast expansion (n=4). Mixed effects analysis was run on the samples. C - Graph showing the mean fluorescence intensity of active integrin β 1 through on day 3 and 5 of expanding erythroblasts and after stimulation with manganese (Mn⁺; n=4). D - Graph showing the mean fluorescence intensity value obtained by flow cytometry of the ephrin-B2 construct binding on days 3 and 5 of expansion of the erythroblasts with 15-minute treatments of either no peptide, a control peptide (DYP) or an EphB4 inhibitor (TNYL) (n=3). E - Graph showing the percentage of cells obtained by flow cytometry expressing the active form of integrin β 1 (clone HUTS-21) on days 3 and 5 of erythroblast expansion with 15-minute treatments of either no peptide, a control peptide (DYP) or an EphB4 inhibitor (TNYL) (n=2). The error bars represent the standard error of the mean. Comparison between the samples was conducted using one-way ANOVA (* p \leq 0.05, NS p \geq 0.05).

Figure 3 - EPHB4 is required for contact inhibition of locomotion in erythroblastic island formation

A – Example of analysis performed on an incucyte experiment with the control peptide, DYP. +Dex macrophages (labelled with Cell Tracker green) were grown from PBMC selected by adherence. The erythroblasts were added at a ratio of 10:1. The excess erythroblasts were gently removed by washing with media after 16 hours incubation. The cells were imaged every hour. Macrophages are individually identified by the program due to their green colour. The programme then recognises at each frame how many erythroblasts (red) are in contact (link) with the identified macrophage. Scale bar is 20µm. B – Min to max boxplot showing the mean duration of links between macrophages and erythroblasts. Kruskal-Wallis test was performed on 2038 macrophages for +Dex EPHB4 inhibitor, 2444 for +Dex Control peptide and 1841 for +Dex VLA-4 inhibitor (n=3). The y-axis is a log₂ scale. C – Min to max boxplot showing the average number of links between macrophages and erythroblasts. Kruskal-Wallis test was performed on 2038 macrophages for +Dex EPHB4 inhibitor, 2444 for +Dex Control peptide and 1841 for +Dex VLA-4 inhibitor (n=3). D - Scaled cell-displacement vector diagrams of macrophage movement for 18 randomly selected macrophages from control peptide and 13 from the EPHB4 inhibitor condition. E - Mean plot of total path length for 82 randomly selected macrophages from control peptide and 46 from EPHB4 inhibitor conditions. Two-tailed t-test run on these samples. NS p≥0.05, **** p≤0.0001.

Figure 4 – Loss of EPHB4, not EPHB6, in erythroblasts impacts macrophage-erythroblast interactions

A – Lysates from day 4 expanding erythroblasts, treated with either scrambled control, EPHB4 or EPHB6 shRNA, and were blotted for EPHB4, EPHB6 and GAPDH. This is a representative plot (n=5). B– Quantification of the blots in A and 4 other repeats (n=5), normalised to GAPDH. Comparison between the samples was done with a two-way ANOVA. C – Graph showing the mean fluorescence value obtained by flow cytometry of the ephrin-B2 construct binding through three days of erythroblast expansion. Erythroblasts were treated with either scrambled, EphB4 or EphB6 shRNA prior to the binding construct experiment (n=4). D – Graph showing the percentage of cells obtained by flow cytometry expressing the active form of integrin β1 (clone HUTS-21) through three days of expansion of shRNA-treated erythroblasts (n=4). Comparison between the samples was done with a two-way ANOVA. E – Min to max boxplot showing the mean duration of links between macrophages and erythroblasts on days 3 and 5 of erythroblast culture. Erythroblasts were transduced with either scrambled, EphB4 or EphB6 shRNA before co-culturing with macrophages and assessment of link formation. Kruskal-Wallis test was performed on 5023 macrophages for scrambled, 6060 for EPHB4 KD, and 3467 for EPHB6 KD (n=3). The y-axis is a log₂ scale. F - Min to max boxplot showing the

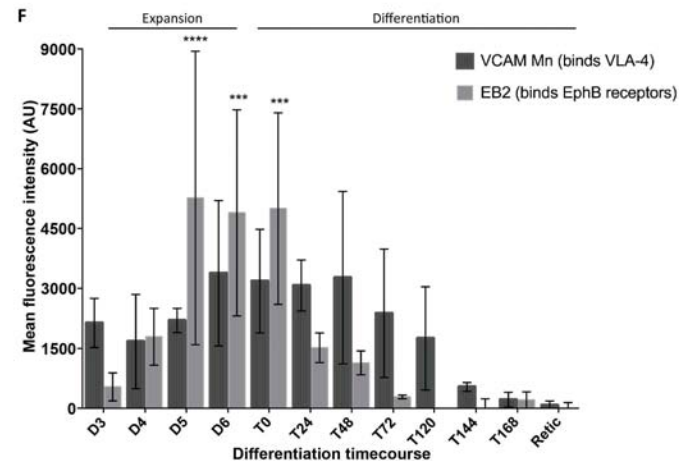
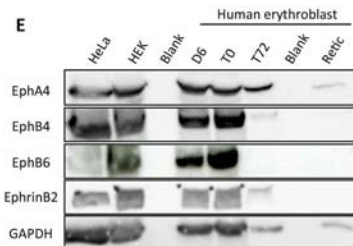
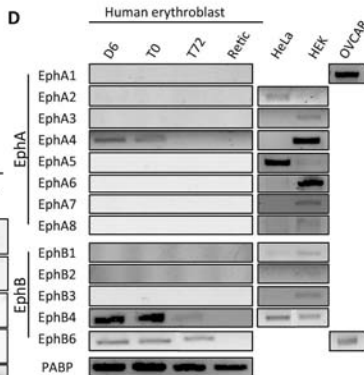
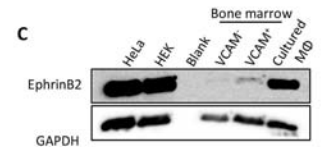
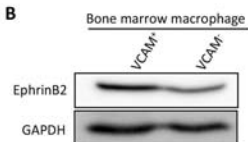
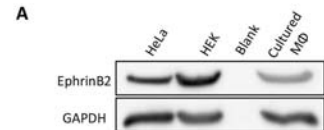
average number of links between macrophages and erythroblasts. Kruskal-Wallis test was performed on 5023 macrophages for Scrambled, 6060 for EPHB4 KD, 3467 for EPHB6 KD (n=3). The y-axis is a log₂ scale. The error bars represent the standard error of the mean, NS p≥0.05, * p≤0.05, **** p≤0.0001.

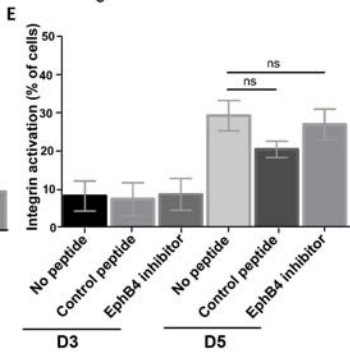
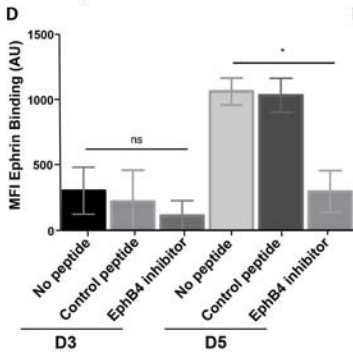
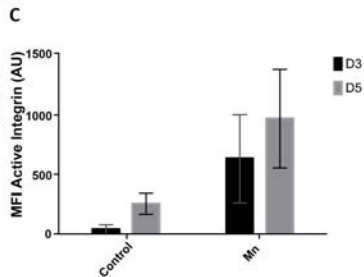
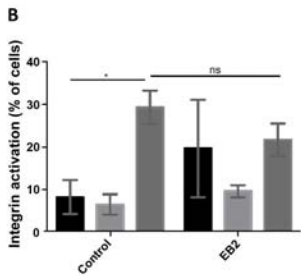
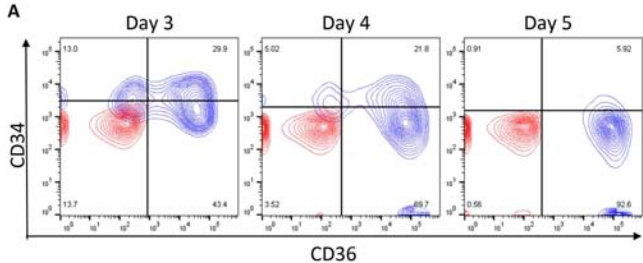
Figure 5 – Bone marrow macrophage-erythroblast interaction is sensitive to EPHB4 and EPHB6 depletion

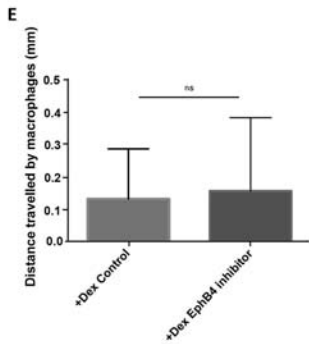
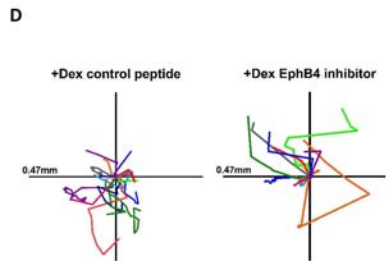
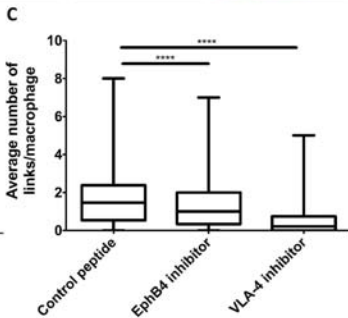
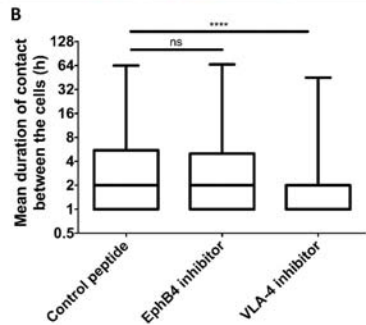
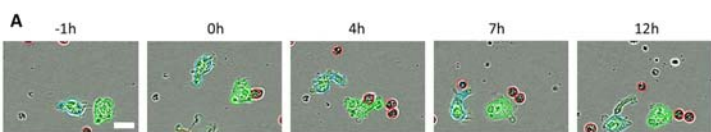
A – Schematic demonstrating workflow for island reconstitution. B – Widefield image of a cluster in a VCAM⁺ sample. M is for the central macrophage and E for erythroblasts. C - Scaled cell-displacement vector diagrams of macrophage movement for 11 randomly selected VCAM⁺ macrophages and 20 VCAM⁻. D - Min to max boxplot showing the mean duration of links between bone marrow macrophages and erythroblasts. Kruskal-Wallis test was performed on 1123 macrophages for scrambled VCAM⁺ cells, 615 for EPHB4 KD VCAM⁺ cells, 647 for EPHB6 KD VCAM⁺ cells, 779 for scrambled VCAM⁻ cells, 164 for EPHB4 KD VCAM⁻ and 432 for EPHB6 KD VCAM⁻ from 2 separate experiments from the same donor. The y-axis is a log₂ scale. E - Min to max boxplot showing the average number of links between bone marrow macrophages and erythroblasts. Kruskal-Wallis test was performed on 1332 macrophages for scrambled VCAM⁺ cells, 875 for EPHB4 KD VCAM⁺ cells, 854 for EPHB6 KD VCAM⁺ cells, 963 for scrambled VCAM⁻ cells, 164 for EPHB4 KD VCAM⁻ and 714 for EPHB6 KD VCAM⁻ from 2 separate experiments from the same donor. The y-axis is a log₂ scale. *** p≤0.001, **** p≤0.0001.

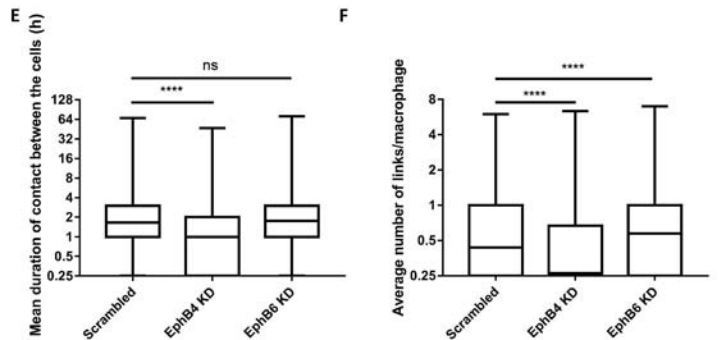
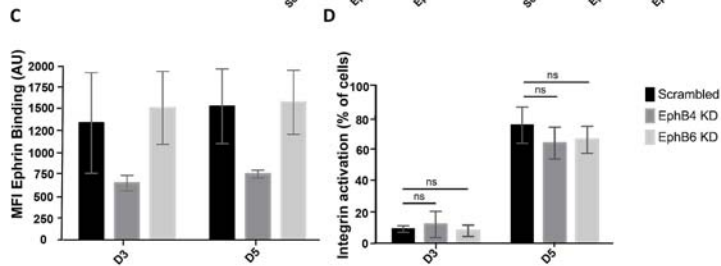
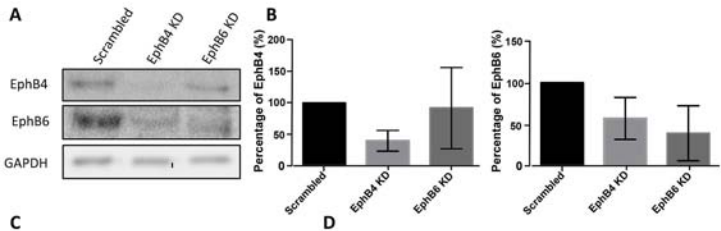
Figure 6 – Schematic for the role of receptors in erythroblastic island development.

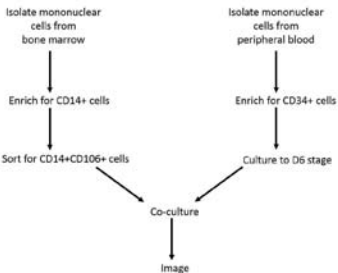
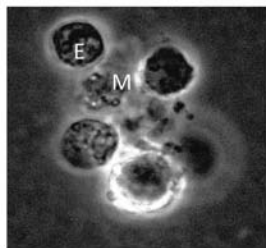
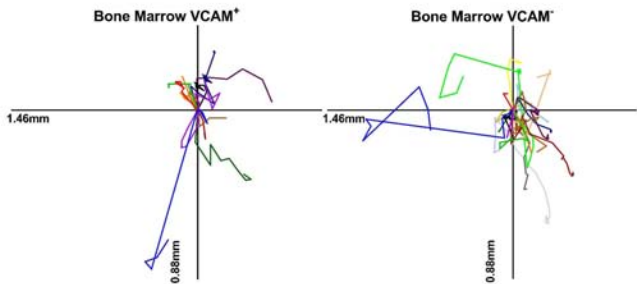
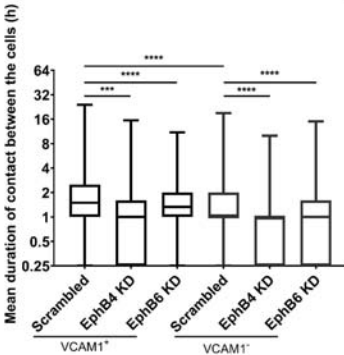
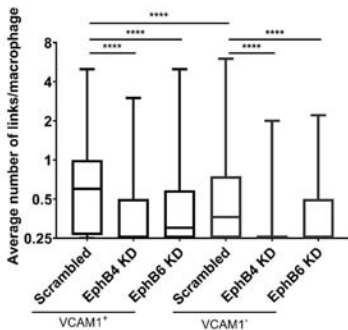
Summary diagram of the receptors involved in macrophage-erythroblast binding in erythroblastic island development in the VCAM⁺ cells of the bone marrow compared to *ex vivo* culture and VCAM⁻ cells.

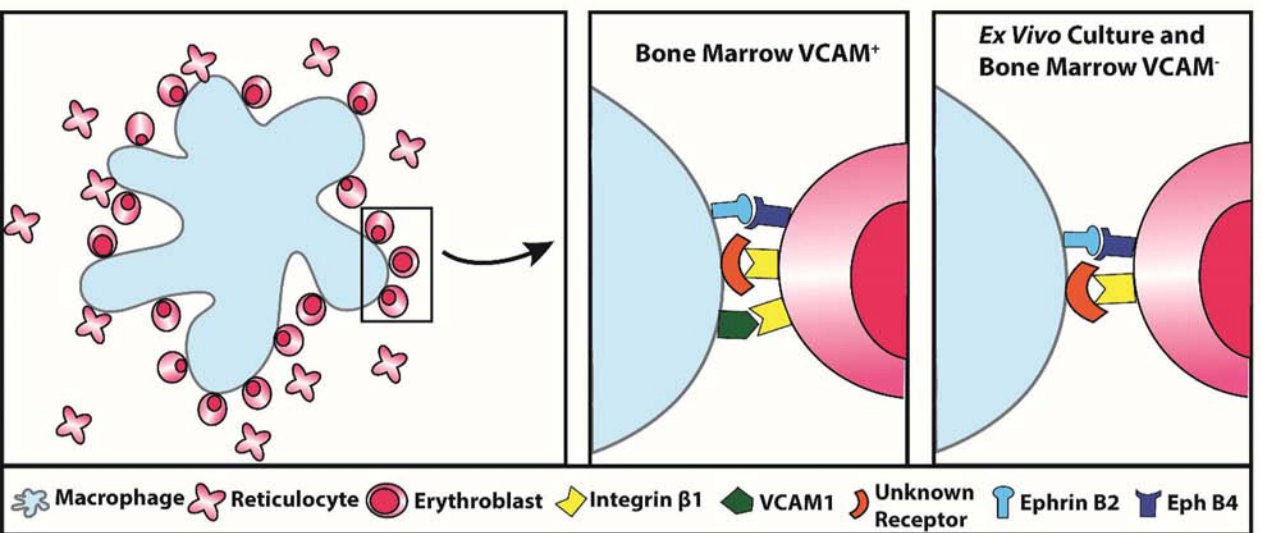


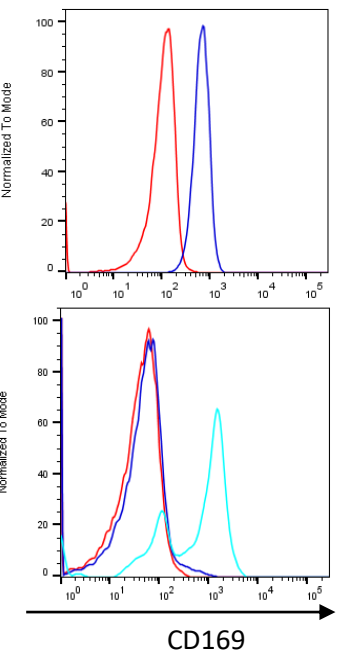
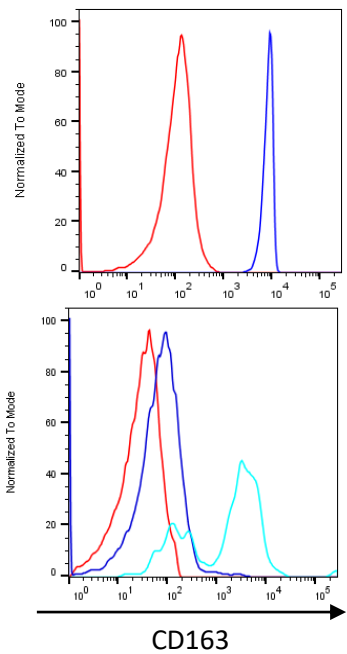
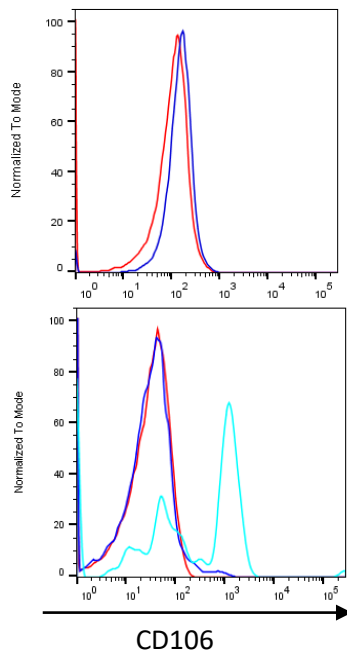
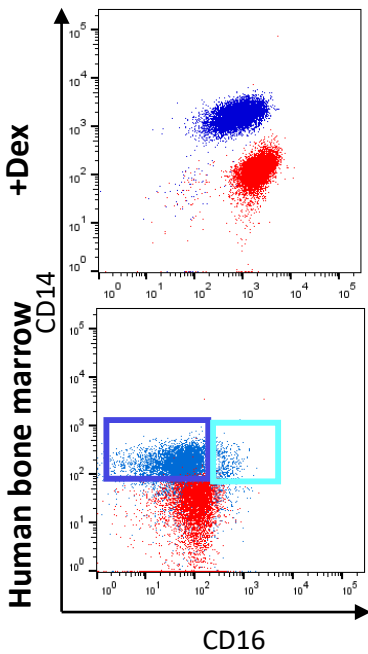






A**B****C****D****E**



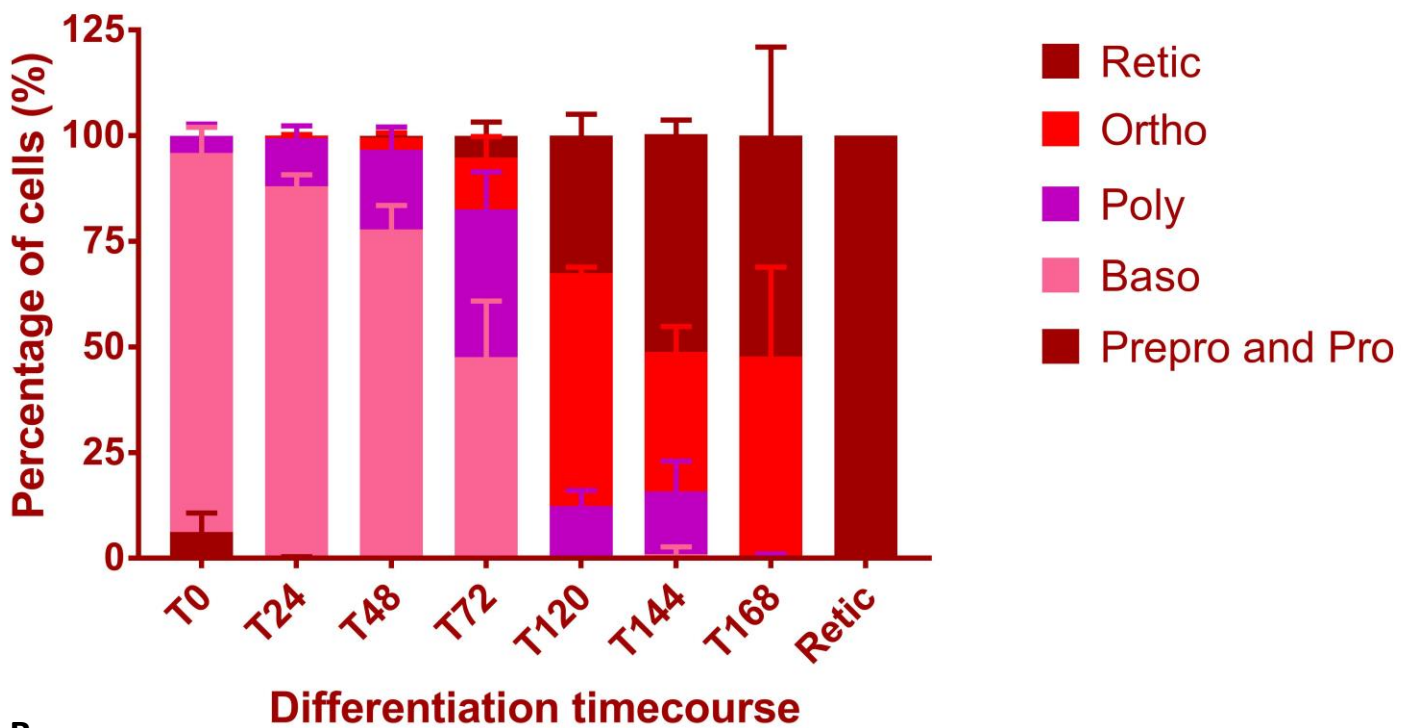
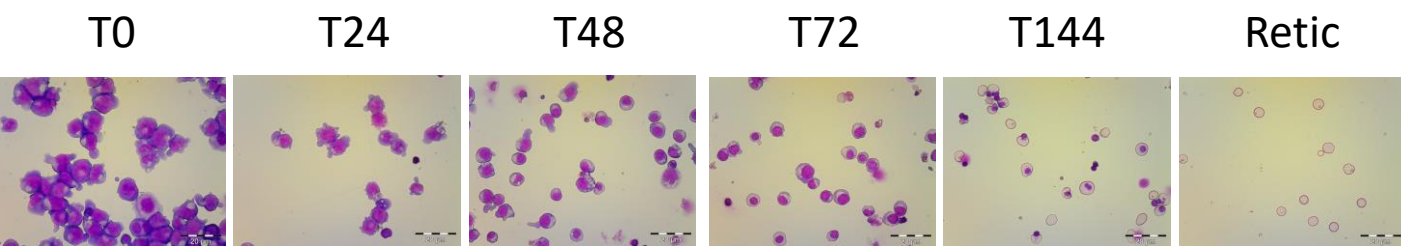


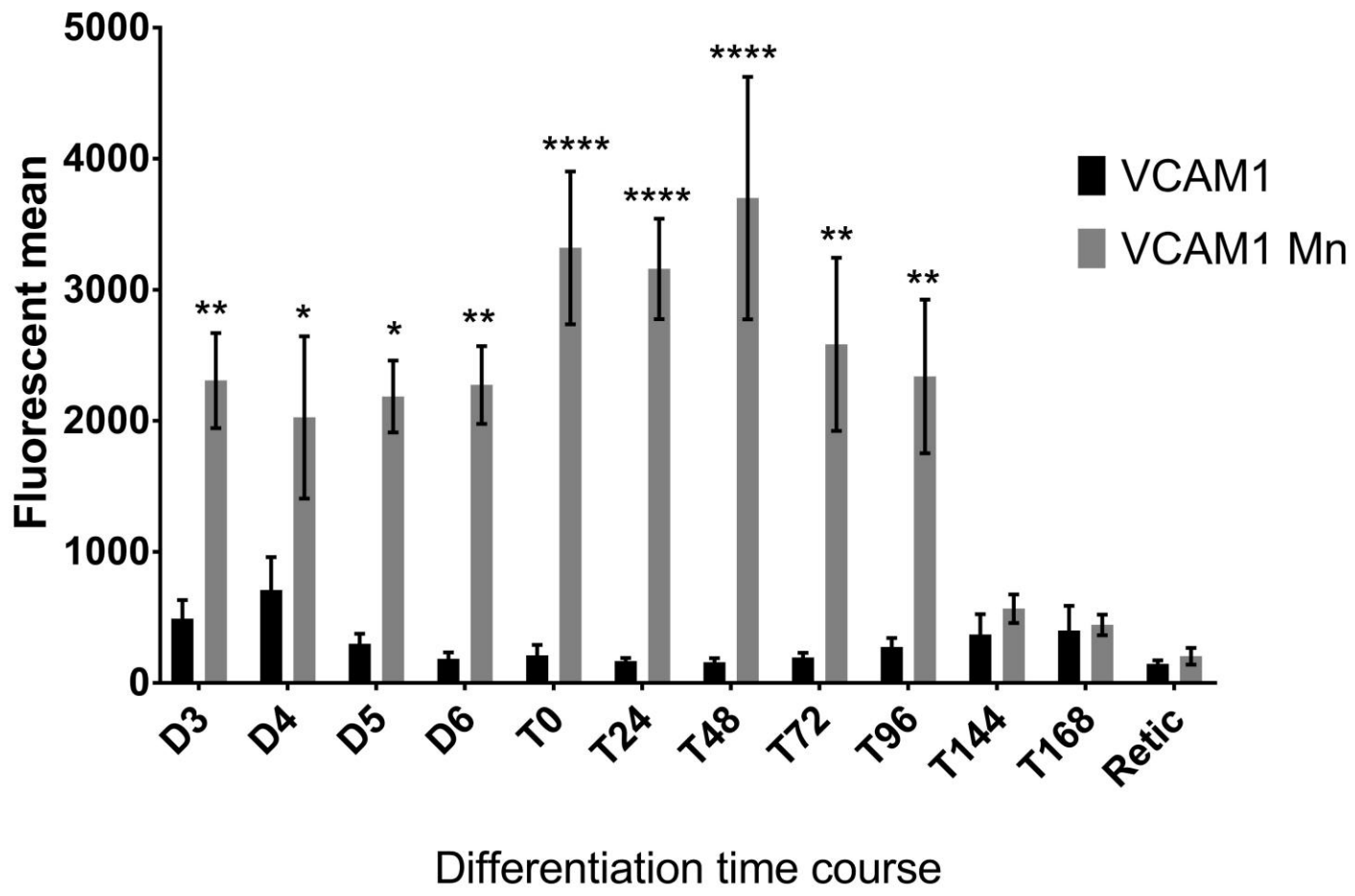
CD16

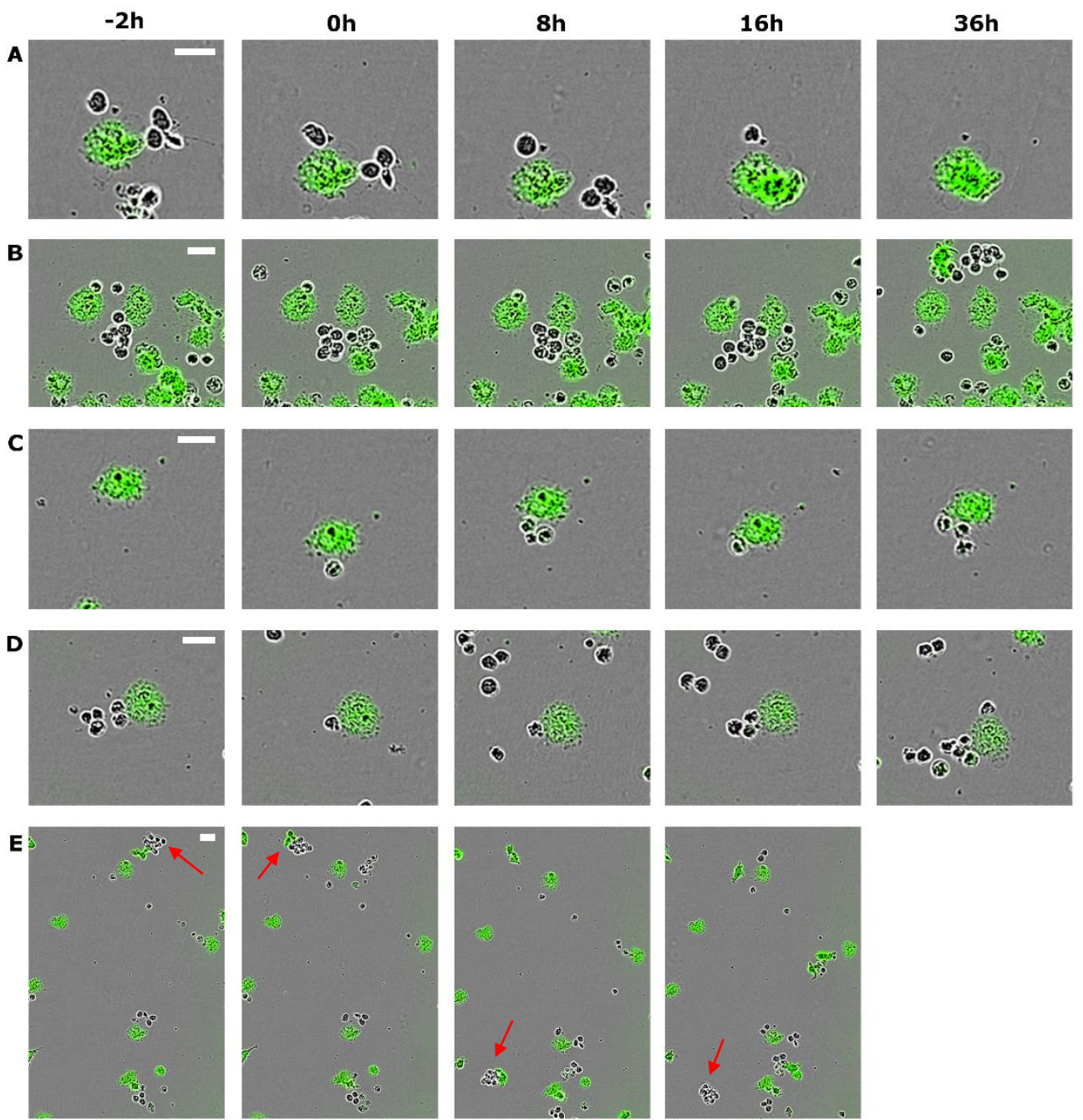
CD106

CD163

CD169

A**B**





-1h

0h

6h

13h

40h

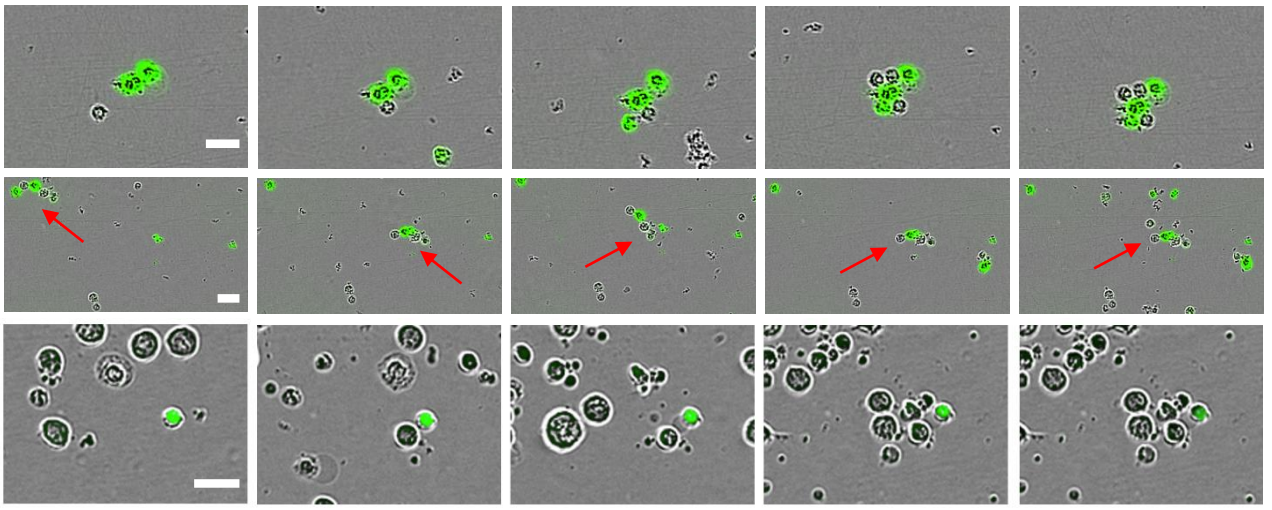


Figure S1 – +Dex macrophages have a similar phenotype to human bone marrow macrophages

Representative flow cytometry histograms of bone marrow macrophage cells and +Dex macrophages stained for CD14, CD16, CD106, CD163 and CD169. Dark blue box and lines are the CD14⁺CD16⁻ cells. The light blue box and lines are the CD14⁺ CD16⁺ cells.

Figure S2 – The different stages of erythropoiesis at different culture points present

A – Cytospins were captured for each day of the culture. 200 cells were categorised in each sample using morphological factors (n=6). B – Example pictures of cytopins for each day of culture.

Figure S3 – VCAM1-Fc binds to the integrins after Mn²⁺ activation

Graph showing the mean fluorescent intensity (MFI) obtained by flow cytometry of the constructs binding to erythroblasts throughout terminal differentiation (n=3). VCAM Mn is VCAM-Fc with manganese activation. The error bars represent the standard error of the mean. 2way ANOVA was performed as a comparison of binding compared to the IgG control (* (p<0.05); ** (p<0.01); **** (p<0.0001)).

Figure S4 - +Dex cells can form transient and long-lasting contacts with erythroblasts

A-E - +Dex macrophages (labelled with Cell Tracker green) were grown from PBMC. The erythroblasts were added at a ratio of 10:1. The excess erythroblasts were gently removed by washing 16 hours after. The cells were imaged every hour. These are examples of cells binding each other either in a transient (A, B and E) or non-transient manner (C and D). The arrow in red in E indicates a macrophage which moves with the erythroblastic cells until it detaches from them. The time indicated is in relation to the cells binding for the first time. Scale bar in all images represents 20µm.

Figure S5 – Bone marrow form these same transient and long-lasting contacts in this method

Bone marrow macrophages (labelled with Cell Tracker green) were sorted for the CD14⁺CD106⁺ cells. The erythroblasts were added at a ratio of 10:1. The excess erythroblasts were gently removed by washing 16 hours after. The cells were imaged every hour. These are examples of cells binding each other in a long-lasting manner. The arrow in red indicates a group of macrophage and erythroblast moving along together. Scale bar in all images represents 20µm.

Antibodies

Monoclonal antibodies used were Pacific Blue conjugated CD14 (BD Pharmingen, Franklin Lakes, New Jersey, US), FITC conjugated CD16 (Miltenyi, Bergisch Gladbach, Germany), PE conjugated CD163 (Miltenyi), APC conjugated CD169 (Miltenyi), PE conjugated CD106 (VCAM1; Biolegend, San Diego, California, US), VioBlue conjugated CD34 (Miltenyi) and PE conjugated CD36 (Miltenyi). Polyclonal mouse anti-EphB6 (Abnova, Taipei City, Taiwan) and rabbit anti-EphA4 (Abcam, Cambridge, UK), anti-GAPDH (Santa Cruz, Dallas, Texas), anti-EphB4 (Novus Biologicals, Abingdon, UK) and anti-ephrin-B2 (Novus Biologicals) were used for immunoblotting. HRP-conjugated rabbit anti-mouse, swine anti-rabbit and rabbit anti-goat (DAKO, Santa Clara, US) for immunoblotting. Monoclonal mouse anti-human CD29 (Clone HUTS-21; BD Pharmingen) was used to detect the active form of integrin β 1 for flow cytometry. Anti-mouse PE secondary was purchased from Biolegend. Recombinant mouse ephrin-B2-Fc chimera protein and recombinant human VCAM1-Fc chimera protein were purchased from R&D systems (Minneapolis, Minnesota, US). Human IgG whole molecule (Jackson ImmunoResearch, West Grove, Pennsylvania, US) were used as a control. Goat anti-human IgG+IgM 647 (Jackson ImmunoResearch) was used to cluster the Fc constructs in the binding experiment.

Human cell culture

HEK293T cells (human embryonic kidney 293 cell line) and HeLa cells were cultured in Dulbecco's Modified Eagle's Medium (DMEM) with GlutaMAX (Invitrogen Ltd, Carlsbad, California, US) containing 10% (v/v) fetal calf serum. Cells were incubated at 37°C in 5% CO₂.

CD34⁺ isolation and culture

Peripheral blood mononuclear cells (PBMCs) were isolated by density purification ($\rho = 1.077$; Percoll; GE Healthcare, Chicago, Illinois) from healthy donors with informed consent given in accordance with the Declaration of Helsinki. The use of human donor peripheral blood progenitors was approved by the Bristol Research Ethics Committee (REC Number 12/SW/0199). Erythroblasts were

expanded and differentiated as described previously³⁵. Reticulocytes were filtered using a 5µm Acrodisk Syringe filter (PALL, Port Washington, New York, US) to remove nuclei and nucleated cells.

Macrophage differentiation

The use of human donor peripheral blood progenitors for production of macrophages was approved by Bristol Research Ethics Committee (REC Number 12/SW/0199). PBMCs were isolated from peripheral blood in the same way as the CD34⁺ cells. These cells are resuspended at a density of 3×10^6 /mL in Roswell Park Memorial Institute media (RPMI; Thermo Fischer, Waltham, Massachusetts, US) supplemented with 100 units/mL penicillin (Sigma-Aldrich, St Louis, Missouri, US), 10% foetal bovine calf serum and 25ng/mL M-CSF (Miltenyi), +/- 1µM dexamethasone (Sigma-Aldrich). The media was changed every third day and the selection for macrophages was conducted by adhesion selection, keeping only adherent cells. The macrophages were considered mature at day 7. To perform flow cytometry, the cells are scraped off the plate before being counted.

Erythroblast EphB4 and EphB6 lentiviral shRNA depletion

pLKO.1 EphB4 and EphB6 shRNA plasmids were designed by the Broad Institute and purchased from GE Healthcare (TRC number TRCN0000001774 for EphB4 knockdown and TRCN0000002018 the EphB6 knockdown). pLKO.1 scrambled was used as the scrambled control. Erythroblasts were transduced with lentivirus as described previously³⁶. Briefly, cultured cells were counted and 0.5×10^6 cells plated in 1mL of appropriate media including polybrene (Sigma-Aldrich) added at 8µg/mL. 50-100µL of concentrated virus was added drop wise to the cells and cells were incubated for 24 hours at 37°C in 5% CO₂. After 24 hours, the virus treated cells were washed 3 times in PBS and re-plated in 2mL of fresh media and cultured as described above. The transfected erythroblasts were selected by puromycin treatment.

RT-PCR

RNA was extracted using the Quick-RNA Microprep (Zymo Research, Irvine, California, US) from 1×10^6 cells at the indicated time point during differentiation. cDNA was synthesised from 100ng

DNase-treated RNA using Superscript III (Invitrogen). Real-time PCR was performed on 1 μ L of cDNA using fast cycling PCR kit (Qiagen, Hilden, Germany).

Western Blotting

Cell pellets of 1 \times 10⁶ cells were lysed in 1% NP-40 lysis buffer. Proteins were resolved by SDS-PAGE and transferred to PVDF (Millipore, Burlington, Massachusetts, US) by western blotting. Membranes were blocked with 5% milk in TBS-T followed by incubation with primary antibodies as indicated in the figure legends followed by HRP-conjugated secondary antibodies. Protein bands were visualized using enhanced chemiluminescence (GE Healthcare) using an Amersham Imager 600 machine.

Flow cytometry and surface binding assay

For the surface binding assay, ephrin-B2-Fc construct or IgG control were pre-clustered at a ratio of 5:1 with Alexa 647 conjugated secondary for 45 minutes at room temperature. Then, 2 \times 10⁴ cells were incubated with the ephrin-B2-Fc construct or IgG control for 30 minutes at 4°C. The cells were washed in PBSAG. For phenotyping the macrophages and erythroblasts, 1 \times 10⁵ cells were incubated with directly conjugated antibodies in cell-type specific panels for 30 minutes at 4°C. Fluorescent signals were measured using a Miltenyi MacsQuant Analyzer 10 flow cytometer. Data was analyzed using FlowJo X.10.6 software (TreeStar Inc, Ashland, Oregon, US).

Cytospins

5 \times 10⁵ cells were cytospun onto glass slides, fixed in methanol, and stained with May-Grünwald-Giemsa stains according to the manufacturer's protocol. Images were taken using an Olympus CX31 microscope coupled to an Olympus LC30 camera using a 40 \times lens and cytospin counts were done by hand using Mousotron (Blacksun Software).

Statistical analysis

The statistical tests were chosen using SPSS (IBM, Armonk, New York, US). Further statistical testing was performed using GraphPad Prism (La Jolla, California, US). The test chosen is indicated in the appropriate figure legend.